

**Influence of charged oxide layers on TEM imaging of reverse-biased  $p$ - $n$  junctions**M. Beleggia,<sup>1,\*</sup> P. F. Fazzini,<sup>1</sup> P.G. Merli,<sup>2</sup> and G. Pozzi<sup>1</sup><sup>1</sup>*Department of Physics and Istituto Nazionale per la Fisica della Materia, University of Bologna, Viale B. Pichat 6/2, 40127 Bologna, Italy*<sup>2</sup>*CNR-IMM, Sezione di Bologna, via P. Gobetti 101, 40129 Bologna, Italy*

(Received 13 November 2002; published 31 January 2003)

Experimental observations of reverse-biased  $p$ - $n$  junctions by means of the out-of-focus method display features which cannot be interpreted within the standard theory of an abrupt  $p$ - $n$  junction. In order to reconcile theory and experiment it is necessary to introduce an active role of the specimen surfaces. In particular it is shown how the introduction of a suitable surface density charge at the interface between the silicon and oxide created after the thinning process allows us to explain the main features of the experimental results. Moreover, some questions left unanswered by previous observations made by Lorentz and holographic methods will be clarified. The results point out that oxide charging cannot be overlooked and should be properly taken into account whenever semiconductor devices are observed by transmission electron microscopy techniques, especially when these methods are employed for the analysis of dopant diffusion in submicron devices.

DOI: 10.1103/PhysRevB.67.045328

PACS number(s): 68.37.Lp, 85.30.De, 85.40.-e

Determination of the two-dimensional (2D) dopant distribution in semiconductor materials at the nanometer scale is one of the most challenging problems that has to be solved in order to make progress towards diminishing device dimensions.<sup>1</sup> It has been remarked by Rau and co-workers<sup>2</sup> that “no technique exists to map the distribution of dopants in two dimensions.” Hence, in order to achieve this aim they applied electron holography to map the 2D depletion layer region of electrostatic potential in submicron transistors, obtaining a 10 nm resolution and 0.1 V sensitivity.

However, further electron holography studies have shown that several problems are still present: for instance, 25 nm “dead layers” at the interfaces of cross-sectional samples,<sup>2</sup> sample charging, thickness corrugations, and strain.<sup>3,4</sup> In order to circumvent these drawbacks and obtain reliable results, researchers have tried to improve specimen preparation techniques,<sup>5–8</sup> including carbon coating of one surface of the specimen in order to remove beam-induced charging.<sup>6</sup>

In our opinion and according to our past experience in this field, it is equally important to better understand the physics of the  $p$ - $n$  junction as observed in the transmission electron microscope. For this task, reverse biasing is essential as it adds another degree of freedom under control of the experimenter.

Our interest in the observation of the electrostatic field associated with reverse-biased  $p$ - $n$  junctions by transmission electron microscopy (TEM) techniques dates to the very beginning. Following the pioneering low-angle electron diffraction experiments by Titchmarsh and Booker,<sup>9</sup> we have shown that reverse-biased  $p$ - $n$  junctions can also be investigated experimentally by out-of-focus and low-angle Foucault methods,<sup>10</sup> by electron interferometry,<sup>11</sup> and finally by electron holography.<sup>12,13</sup> These studies have led us to appreciate the fact that the effect of the electrostatic field around the specimen is by no means negligible,<sup>10</sup> but may become the predominant factor contributing to the electron optical phase shift.<sup>14</sup> Therefore, theoretical analysis and modeling both play a relevant role in taking into account the external field.

The problem of the fringing field and its associated electron optical phase shift has been solved for the case of straight junctions in an infinite specimen described by the one-sided step model both numerically<sup>15</sup> and analytically.<sup>16</sup> Moreover, the observations are usually carried out near a hole in the specimen and this fact gives rise to a more difficult boundary value problem. Recently, an analytical solution has been found for the electrostatic potential generated by an array of  $p$  and  $n$  stripes perpendicular to the edge in a semi-infinite specimen.<sup>17</sup> Therefore, it is now possible to interpret images of junctions near the edge and investigate how they are influenced by it. This model has also been extended to cover the case of the junction tilted with respect to the specimen edge.<sup>18</sup> The simulations show that the out-of-focus images (but not the holographic ones) are only affected in the immediate proximity of the edge. Hence, the adoption of simpler one-dimensional models (still taking into account the external fields above and below the specimen) is justified in order to interpret straight reverse-biased  $p$ - $n$  junction images far from the edge itself.

Having developed a theoretical framework able to cope with realistic specimen geometries, we have recently tested it against experiments, obtaining disappointing results.<sup>19</sup> The deduction of the theoretical input data from the standard bulk theory of  $p$ - $n$  junctions<sup>20</sup> failed to properly interpret the experimental results. Furthermore, in the thinner parts of the specimen, the junction contrast did not reach the specimen edge and the presence of an anomalous contrast line indicated the existence of an inversion layer, confirming earlier experimental findings.<sup>10,11</sup> These facts, combined with the results of previous electron holography experiments,<sup>13</sup> where the built-in potential was not detected in spite of the sufficient sensitivity of the method (similar results with unbiased specimens have been obtained also by other authors<sup>2,5,6,8</sup>), prompted us to improve the existing theoretical model.

We have therefore considered the hitherto neglected influence of the finite specimen thickness, surface states, and beam-induced charging of the oxide layers on the field topography using a professional CAD software (in our case the

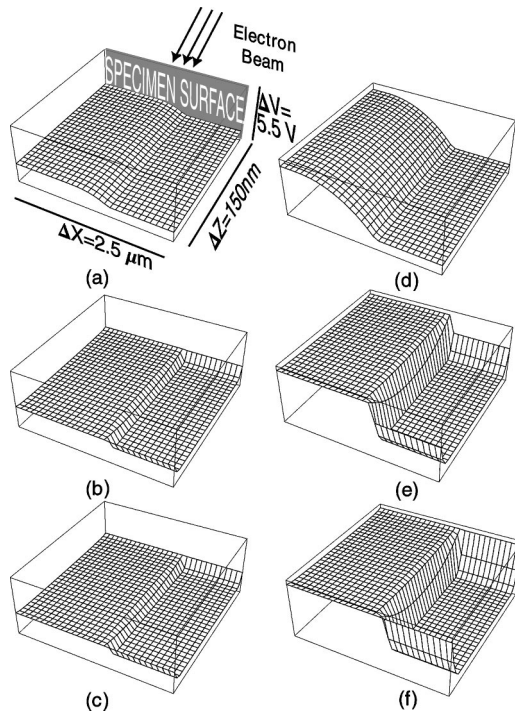


FIG. 1. Two-dimensional simulated map of the internal potential distribution in the thinned specimens. The arrows in (a) indicate the impinging electron beam direction. Specimen is unbiased in (a),(b),(c) and reverse biased at 3V in (d),(e),(f). Surface density charge values used for simulations were 0 e.c./cm<sup>2</sup> in (a),(d)  $2.5 \times 10^{13}$  e.c./cm<sup>2</sup> in (b),(e), and  $5 \times 10^{13}$  e.c./cm<sup>2</sup> in (c),(f).

ISE-TCad), which is specially designed for simulating the behavior of semiconducting devices.<sup>21</sup> The first theoretical results showed that neither the finite specimen thickness nor the presence of Shockley-Read-Hall states at the silicon-vacuum interfaces affected the internal and external electrostatic field topographies. On the contrary, the field topographies are strongly influenced by the introduction of surface charges in the range  $10^{13}$ – $10^{14}$  e.c. (electron charges)/cm<sup>2</sup>.

In the present work, further consequences of this hypothesis are examined and tested against experiment. At first the effects of the surface charge on the internal potential distribution across a *p-n* junction arising between two regions having constant doping of  $5 \times 10^{15}$  cm<sup>-3</sup> (*n* region) and  $2 \times 10^{19}$  cm<sup>-3</sup> (*p* region) are investigated.

Figure 1 shows the simulated potential, plotted along  $2.5 \mu\text{m}$  of a 150-nm-thick specimen [one of the specimen surfaces is indicated for clarity in (a)], for the cases of 0 V (left column) and 3 V (right column) reverse bias. Figures 1(a) and 1(d) show the potential distribution across the junction when no surface charge is present and represent the ideal reference case. When a charge density of  $2.5 \times 10^{13}$  e.c./cm<sup>2</sup> is added, it can be seen that the junction profile inside the specimen is steeper (b), (e), while the potential difference at the surfaces almost vanishes when the reverse bias is 0 V (b), meaning that no external fringing field is present, contrary to the uncharged case. By applying the reverse bias the potential difference at the surface is partly recovered, so that the external fringing field is now

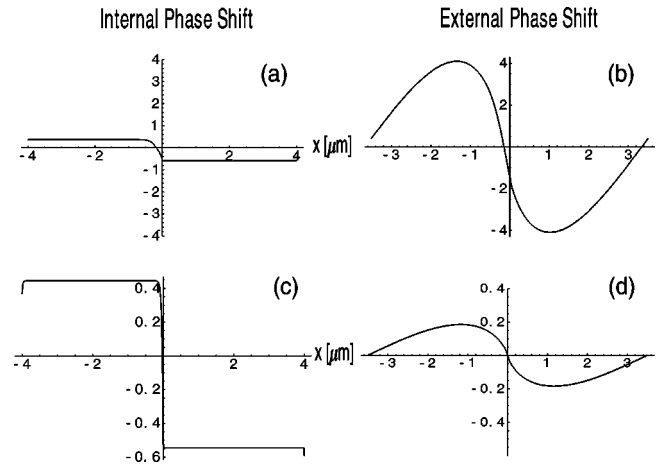


FIG. 2. External and internal phase contributions. Surface density charge is 0 in (a),(b) and  $2.5 \times 10^{13}$  e.c./cm<sup>2</sup> in (c),(d).

present (e). By further increasing the charge density up to  $5 \times 10^{13}$  e.c./cm<sup>2</sup> the external field becomes again negligible, both in the unbiased (c) and biased (f) conditions.

The presence of surface charges explains the absence of the external field associated with the built-in potential already noted in several holography experiments.<sup>2,7</sup> It must be pointed out that in some cases the effects of the external field are not observed even when the specimen is reverse biased.<sup>7</sup> Figure 2 shows the influence of external and internal phase contributions in the unperturbed (a),(b) and charged (c),(d) cases. It can be seen that when there is no charge at the interfaces the external field contribution is an order of magnitude stronger than the internal one, and so cannot be neglected, especially in holography experiments.

The drastic changes of both the internal and external fields strongly depend on the surface charge density and affect in a substantial way the phase shift experienced by the electrons in a TEM experiment. In particular, some calculations show that it is possible to discriminate between different junction models also by means of the out-of-focus method in spite of its shortcomings for obtaining truly quantitative results.<sup>22</sup>

Out-of-focus observations of reverse-biased *p-n* junctions have been carried out using a Tecnai F20, equipped with a Schottky emitter. The pertinent experimental conditions were as follows: 200 kV accelerating voltage and illumination crossover approximately 20 cm above the specimen, obtained by switching off the second condenser, microcondenser, and objective lens with a suitable setting of the first condenser. In these conditions the angular resolving power was better than  $1 \times 10^{-6}$  rad. The imaging system provided by the diffraction, intermediate, and projector lenses controlled the out-of-focus distance and the specimen magnification, which were carefully calibrated by three independent methods: (1) the analysis of the spectrum of a shadowed carbon grating, which displays rings whose spacing is related to the defocus, (2) the realization of a low-angle diffraction image by varying only the condenser lens, and (3) the analysis of the Fresnel edge diffraction fringes.<sup>23</sup>

The scheme of the diode is shown in Fig. 3. The junction was obtained by deposition of Boron on an *n*-doped Si sub-

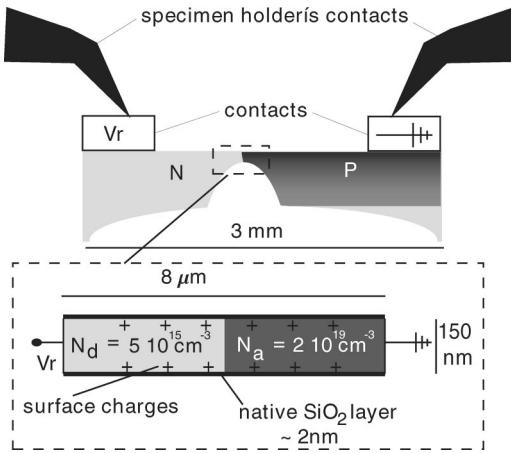


FIG. 3. Schematic view of the diode used in the observation and of its modeling in numerical device simulations.

strate followed by thermal annealing, resulting in a  $p^+ - n$  junction whose approximate dopant concentrations are  $N_d = 5 \times 10^{15} \text{ cm}^{-3}$  and  $N_a = 2 \times 10^{19} \text{ cm}^{-3}$ . The specimen was prepared for TEM in two steps: first it was mechanically thinned using a dimple grinder and then ion milled until a hole across the junction was formed.

Observations have been carried out at various reverse bias and defocuses. We report in Fig. 4 out-of-focus images taken in a region of the specimen having thickness 150 nm (measured by convergent beam electron diffraction) at two defocus distances: +52 mm (a),(b),(c) and -70 mm (d),(e),(f). The reverse bias was 0 V (a),(d), 1.5 V (b),(e), and 3.0 V (c),(f). The regions displayed are far from the edge, in order to diminish its effects, and the overall uniformity of the contrast features over the displayed area confirms that the junction can be safely analyzed by one-dimensional models.

The theoretical images have been calculated using the Kirchhoff-Fresnel diffraction integral by considering both

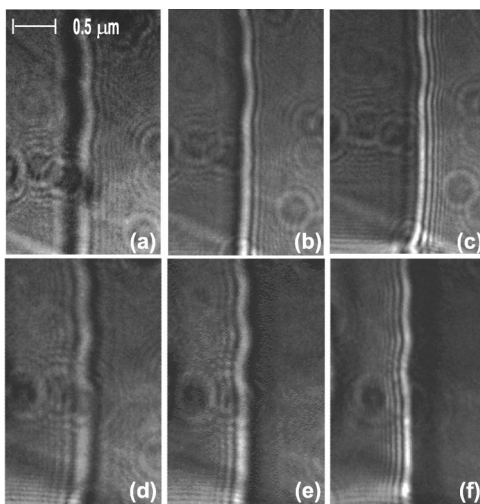


FIG. 4. Out-of-focus images of the  $p - n$  diode. Defocus distances:  $52 \pm 5$  mm in (a),(b),(c) and  $-70 \pm 3$  mm in (d),(e),(f). Reverse bias is  $0 \text{ V} \pm 1\%$  in (a),(d),  $1.5 \text{ V} \pm 1\%$  in (b),(e), and  $3 \text{ V} \pm 1\%$  in (c),(f).

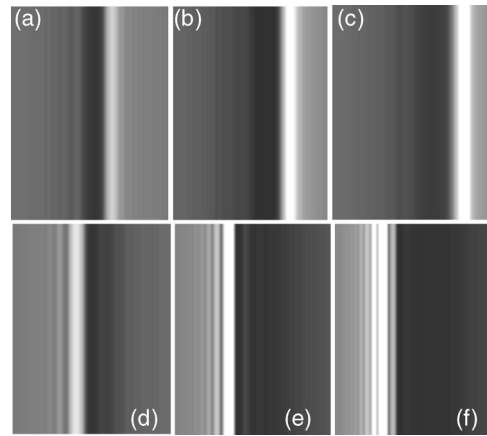


FIG. 5. Image simulations with a surface charge of  $0 \text{ e.c./cm}^2$ . Experimental conditions (defocus distances, magnification, and applied bias) in (a)–(f) are the same as in Figs. 4(a)–4(f).

the internal and external field contributions to the phase shift extracted from the simulation program used for Figs. 1 and 2, assuming a constant thickness of 150 nm. Figure 5 reports the simulations, displayed as density maps, in the same experimental conditions reported in Fig. 4, and neglecting the surface charge. Moreover, partial coherence effects have been taken into account, by considering an illumination aperture of  $8 \times 10^{-7}$  rad. The comparison with the experimental data confirms our previous findings that the simple one-sided step model is unable to interpret the main features of the patterns, especially when a reverse bias is applied.<sup>19</sup>

On the contrary, the simulations carried out for a surface charge density of  $2.5 \times 10^{13} \text{ e.c./cm}^2$ , reported in Fig. 6, again for the same experimental conditions, show a satisfying agreement over the whole potential and defocus ranges. We have also carried out simulations by varying the surface charge density, and agreement between theory and experiment is maintained over the range  $1.5 - 3 \times 10^{13} \text{ e.c./cm}^2$ .

In conclusion, we have shown that the interpretation of the out-of-focus images calls for the introduction of a surface charge density in the model of a thinned  $p - n$  junction. Furthermore, the comparison between theoretical and experi-

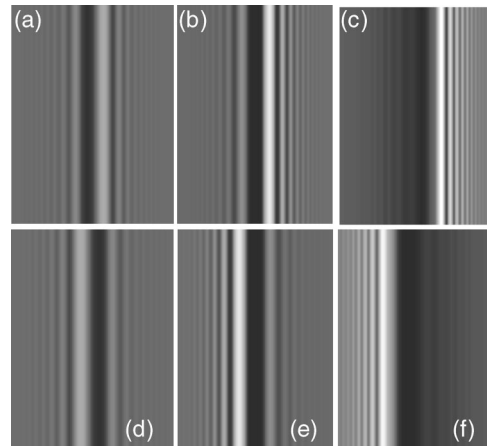


FIG. 6. As in Fig. 5 but with a surface charge of  $2.5 \times 10^{13} \text{ e.c./cm}^2$ .

mental results shows a satisfactory agreement over the whole defocus and potential range investigated only for the charged case, provided the charge density is in the range  $1.5\text{--}3 \times 10^{13}$  e.c./cm<sup>2</sup>.

As a final remark it is worth noting that the presence of surface charges involves a dramatic decrease of the external field. It is our opinion that the external field associated with the built-in potential has not been observed in holography experiments for this reason. The essential role played by the reverse biasing of the junctions and of defocusing in opposite

directions should be noted. In fact, it emphasizes the difference between the models and allows their discrimination.

Work is in progress in order to improve the model of the doping, hitherto assumed to vary abruptly between the *n* and *p* regions, and to ascertain whether a better agreement can be obtained in this way.

Useful discussions with Dr. S. Solmi, Dr. A. Roncaglia, and Dr. P. Maccagnani and the technical assistance of R. Lotti and S. Patuelli are gratefully acknowledged.

---

\*Current address: Materials Science Department, Brookhaven National Laboratory, Upton, NY 11973.

<sup>1</sup>*International Roadmap for Semiconductors*, 2001 ed. (Semiconductors Industry Association, San Jose, CA, 2001); <http://public.itrs.nrt/>

<sup>2</sup>W.D. Rau *et al.*, Phys. Rev. Lett. **82**, 2614 (1999).

<sup>3</sup>R.E. Dunin-Borkowski *et al.*, in *Proceedings of the 12th European Congress on Electron Microscopy, Brno, 2000*, edited by P. Tomanek and R. Kolarik (Czechoslovak Society for Electron Microscopy, Brno, 2000), pp. I63–I64.

<sup>4</sup>A.C. Twitchett and P.A. Midgley, in *Microscopy of Semiconducting Materials 2001: Proceedings of the 12th International Conference on Microscopy of Semiconducting Materials, Oxford University, 25–29 March 2001*, edited by A. G. Cullis and J. L. Hutchison, Inst. Phys. Conf. Ser. No. 169, p. 29 (2001) (IOP, Bristol, 2001).

<sup>5</sup>Z. Wang *et al.*, Appl. Phys. Lett. **80**, 246 (2002).

<sup>6</sup>M.R. McCartney *et al.*, Appl. Phys. Lett. **80**, 3213 (2002).

<sup>7</sup>A.C. Twitchett *et al.*, Phys. Rev. Lett. **88**, 238302 (2002).

<sup>8</sup>M.A. Gribelyuk *et al.*, Phys. Rev. Lett. **89**, 025502 (2002).

<sup>9</sup>J.M. Titchmarsh and G.R. Booker, in *Proceedings of the Fifth European Congress on Electron Microscopy*, edited by V. E. Cosslett (The Institute of Physics Publisher, London and Bristol, 1972) pp. 540–541.

<sup>10</sup>P.G. Merli *et al.*, Phys. Status Solidi A **30**, 699 (1975).

<sup>11</sup>P.G. Merli *et al.*, J. Microsc. (Paris) **21**, 11 (1974).

<sup>12</sup>S. Frabboni *et al.*, Phys. Rev. Lett. **55**, 2196 (1985).

<sup>13</sup>S. Frabboni *et al.*, Ultramicroscopy **23**, 29 (1987).

<sup>14</sup>C. Capiluppi *et al.*, Opt. Spectra **47**, 205 (1977).

<sup>15</sup>G. Pozzi, Optik (Stuttgart) **53**, 381 (1979).

<sup>16</sup>M. Vanzi, Optik (Stuttgart) **68**, 319 (1984).

<sup>17</sup>C. Capiluppi *et al.*, Microsc. Microanal. Microstruct. **6**, 647 (1995).

<sup>18</sup>M. Beleggia *et al.*, Philos. Mag. B **80**, 1071 (2000).

<sup>19</sup>M. Beleggia *et al.*, Micron **31**, 231 (2000).

<sup>20</sup>A.S. Grove, *Physics and Technology of Semiconductor Devices* (Wiley, New York, 1962).

<sup>21</sup>M. Beleggia *et al.*, *Proceedings of the 12th International Conference on Microscopy of Semiconducting Materials, Oxford University, 25–29 March 2001*, edited by A. G. Cullis and J. L. Hutchison, Inst. Phys. Conf. Ser. No. 169, p. 427 (2001) (IOP, Bristol, 2001).

<sup>22</sup>J.N. Chapman, J. Phys. D **17**, 623 (1984).

<sup>23</sup>P.F. Fazzini *et al.*, in *Proceedings of the 15th International Congress on Electron Microscopy, Durban, 2002*, edited by J. Engelbrecht, T. Sewell, M. Witcomb, and R. Cross (Publ. Microscopy Society of Southern Africa, Durban, 2002).